

Segmentation of Substantia Nigra for the Automated Characterization of Parkinson's Disease

Dibash Basukala

Department of Computer Science and
Software Engineering,
University of Canterbury
Christchurch, New Zealand
dibash.basukala@pg.canterbury.ac.nz

Ramakrishnan Mukundan

Department of Computer Science and
Software Engineering,
University of Canterbury
Christchurch, New Zealand
mukundan@canterbury.ac.nz

Tracy Melzer

New Zealand Brain Research Institute,
Department of Medicine,
University of Otago
Christchurch, New Zealand
tracy.melzer@otago.ac.nz

Ross Keenan

New Zealand Brain Research Institute,
Pacific Radiology
Christchurch, New Zealand
ross.keenan@pacificradiology.com

Abstract— Segmentation of smaller brainstem nuclei like substantia nigra (SN) is one of the first stage in computer-aided diagnosis to investigate the Parkinson's disease (PD) characteristics and progression. PD patients generally have smaller SN in comparison to healthy individuals. There are very few automated methods proposed for SN segmentation and most of them require quite a few number of reference images for increasing the accuracy. Therefore, we propose an improved algorithm for the segmentation of SN using level set method and dual-tree complex wavelet transform (DT-CWT). The proposed level set method uses the local image information and maintains the regularity of the level set function for accurate computation, thus precluding the expensive re-initialization process. DT-CWT is used to solve the problem of over-segmentation, also resulting in holes, and to smooth the jagged outputs generated by the level set method. The experimental results suggest that the proposed algorithm is able to segment SN and is closer to manual delineation.

Keywords— Segmentation, Parkinson's disease, level set method, wavelet transform, substantia nigra.

I. INTRODUCTION

Parkinson's disease (PD) is related to the degeneration of neurons in the substantia nigra (SN) pars compacta [1]. The neurons in the SN produce an important brain chemical called dopamine (DA), which plays a vital role in neurotransmission between the SN and corpus striatum for producing smooth purposeful movement. The biochemical imbalance of DA results in poor balance and motor coordination [2], rigidity, resting tremor and bradykinesia (gradual slowness in spontaneous movement). Almost 60 to 80 percent of the DA producing cells in the SN will be lost by the time clinical symptoms start to appear. However, the cause of this cellular death is only partially understood. Hence, detecting SN damage at the early stage will be helpful for identifying the individuals at risk for PD.

Magnetic resonance imaging (MRI) at 7T, a high resolution imaging improves the quality of MR images by utilizing the higher signal-to-noise ratio. Hence, smaller brainstem nuclei like SN can be properly imaged with the

help of this recent advancements. Additionally, the usage of gradient echo (GRE) sequences helps in characterizing SN which contains relatively high iron content [3, 4]. SN is not clearly visible in T1-weighted images while it is readily visible in T2-weighted images and T2*-weighted images because of the presence of iron.

SN located in the midbrain is of particular importance to both clinicians and researchers as it is highly correlated with PD. Menke et al. [5] reported that PD subjects had significantly smaller SN compared to controls. Therefore, accurate segmentation of SN can provide insight to different stages of PD but is challenging, because of its smaller structure and similar intensity value with the peripheral areas. Manual segmentation of SN is tedious and time consuming task and it is susceptible to inter and intra-observer variabilities. Hence, automatic segmentation is preferred to manual segmentation. A fairly limited number of literature is available for the automatic segmentation of SN because high quality imaging capable of visualizing SN is developed lately.

Xiao et al. [6] proposed the atlas based segmentation by combining the T1-weighted and T2*-weighted images for better visualization of the smaller nuclei. Haegelen et al. [7] compared the manual segmentation of deep brain structures with symmetric image normalization (Syn), automatic nonlinear image matching and anatomical labelling (ANIMAL) and a patch based method. Xiao et al. [8] used label-fusion segmentation approach and principal component analysis (PCA) to investigate the morphometric variability of the midbrain nuclei. Kim et al. [9] proposed the semiautomatic segmentation of brain subcortical structures using active surface model and prior shape knowledge. Li et al. [10] proposed the automated segmentation of smaller brain nuclei using level set method. Visser et al. [11] proposed the automated segmentation of the smaller deep brain nuclei using the intensity model and a shape model based on Markov random field (MRF). Similarly, Guo et al. [12] proposed the method based on seed points discontinuity and level set method for the segmentation of cerebral nuclei.

Level set methods are often used for the segmentation of smaller structures in medical image domain. Li et al. [13] proposed the level set method using the region scalable

fitting (RSF) energy for the segmentation of images with intensity inhomogeneities. Similarly, Li et al. [14] proposed a level set method based on the local intensity clustering property which is capable of handling images with intensity inhomogeneities.

However, the methods proposed in existing literature have some limitations. Most of the proposed work for the automatic segmentation of SN are atlas based, template based, label fusion based and prior shape model based. These models require substantial number of reference images to increase the segmentation accuracy but the results are still not error-prone. Moreover, it is also computationally expensive. Therefore, the objective of this study is to present a new and improved algorithm by using level set method and dual-tree complex wavelet transform (DT-CWT) for the accurate segmentation of the SN in T2*-weighted images. This will be helpful for clinicians in the diagnosis of PD.

II. MATERIALS AND METHODS

This research uses the MRI data repository which is freely available and described by Forstmann et al. [15]. The data in the repository were obtained from 53 healthy individuals; 30 young, 14 middle-aged and 9 elderly participants. The data were obtained using a 7 T Siemens Magnetom MRI scanner using a 24-channel head array Nova coil (NOVA Medical Inc., Wilmington MA). The multi-echo 3D FLASH consisted of 128 slices with repetition time (TR) = 41 ms, three echo times (TE): 11.22/20.39/29.57 ms, bandwidth = 160 Hz/Px, flip angle = 14°, voxel size = (0.5 mm)³ and was tilted at -23 degrees.

A. Level set method

Level set method originally proposed by Osher and Sethian [16] is a popular technique for capturing the evolution of dynamic interfaces. It represents the interfaces or contours as the zero level set of a higher dimensional function, usually known as a level set function. Level set method is capable of handling the changes in topology of the interface and shapes in a natural way.

Chan and Vese (CV) [17] proposed the level set method based on Mumford-Shah model [18] for minimizing the energy given by,

$$F^{CV}(C, c_1, c_2) = \lambda_1 \int_{\Omega_1} |I(x) - c_1|^2 dx + \lambda_2 \int_{\Omega_2} |I(x) - c_2|^2 dx + \nu |C| \quad (1)$$

where $\nu \geq 0$, $\lambda_1, \lambda_2 > 0$, Ω_1 is the region outside contour C and Ω_2 is the region inside contour C . c_1 and c_2 approximate the image intensity in Ω_1 and Ω_2 respectively. However, CV model could not segment images with intensity inhomogeneities which are common in medical images.

Hence, Li et al. [13, 19] proposed a model which is capable of segmenting images with intensity inhomogeneities by embedding the local image information. The energy functional in this case is given by,

$$\mathcal{E}(C, f_1(x), f_2(x)) = \int \mathcal{E}_x^{Fit}(C, f_1(x), f_2(x)) dx + \nu |C| \quad (2)$$

where,

$$\mathcal{E}_x^{Fit}(C, f_1(x), f_2(x)) = \sum_{i=1}^2 \lambda_i \int_{\Omega_i} K_\sigma(x-y) |I(y) - f_i(x)|^2 dy \quad (3)$$

is the local intensity fitting energy. $f_1(x)$ and $f_2(x)$ approximate the local intensities in Ω_1 and Ω_2 respectively.

K_σ is a Gaussian kernel in n -D given by,

$$K_\sigma(u) = \frac{1}{(2\pi)^{n/2} \sigma^n} e^{-|u|^2/2\sigma^2} \quad (4)$$

where the scale parameter $\sigma > 0$. The Gaussian kernel with a scale parameter allows the intensity information to be used from smaller neighborhoods to the entire image domain.

In level set methods, $C \subset \Omega$ is represented by the zero level set of a level set function $\phi : \Omega \rightarrow \mathfrak{R}$. Then, (2) can be expressed in the form of level set function ϕ as,

$$\mathcal{E}_\varepsilon(\phi, f_1, f_2) = \sum_{i=1}^2 \lambda_i \int \left(\int K_\sigma(x-y) |I(y) - f_i(x)|^2 M_i^\varepsilon(\phi(y)) dy \right) dx + \nu \int |\nabla H_\varepsilon(\phi(x))| dx \quad (5)$$

where H_ε is a smooth Heaviside function, $M_1^\varepsilon(\phi) = H_\varepsilon(\phi)$ and $M_2^\varepsilon(\phi) = 1 - H_\varepsilon(\phi)$. The entire energy functional is given by,

$$F(\phi, f_1, f_2) = \mathcal{E}_\varepsilon(\phi, f_1, f_2) + \mu P(\phi) \quad (6)$$

where,

$$P(\phi) = \int \frac{1}{2} (|\nabla \phi(x)| - 1)^2 dx \quad (7)$$

is a level set regularization term. Then, the minimization of energy functional $F(\phi, f_1, f_2)$ is performed with respect to ϕ by the gradient descent method,

$$\frac{\partial \phi}{\partial t} = -\delta_\varepsilon(\phi) (\lambda_1 e_1 - \lambda_2 e_2) + \nu \delta_\varepsilon(\phi) \operatorname{div} \left(\frac{\nabla \phi}{|\nabla \phi|} \right) + \mu \left(\nabla^2 \phi - \operatorname{div} \left(\frac{\nabla \phi}{|\nabla \phi|} \right) \right) \quad (8)$$

where δ_ε is the smoothed Dirac delta function,

$$\begin{cases} e_1(x) = \int K_\sigma(y-x) |I(x) - f_1(y)|^2 dy \\ e_2(x) = \int K_\sigma(y-x) |I(x) - f_2(y)|^2 dy \end{cases} \quad (9)$$

and,

$$\begin{cases} f_1(x) = \frac{K_\sigma * [H_\varepsilon(\phi)I]}{K_\sigma * H_\varepsilon(\phi)} \\ f_2(x) = \frac{K_\sigma * [(1-H_\varepsilon(\phi))I]}{K_\sigma * (1-H_\varepsilon(\phi))} \end{cases} \quad (10)$$

In the proposed level set method, we aim to solve level set evolution equation given by (8). The first term in (8) drives the active contour towards the boundaries of the object while the second term maintains the regularity of the contour. The third term which is called as level set regularization term avoids the time-consuming re-initialization process since it maintains the regularity of the level set function which is significant for accurate computation and stable evolution in level set methods.

B. Wavelet transform

Wavelet transform is one of the most popular method for smoothing the images [20]. In our work, we use DT-CWT. In wavelet based methods, smoothing is done by using a threshold for removing high frequency subband coefficients. Thresholding can be performed either by hard or soft thresholding method.

Dual-tree complex wavelet transform

Dual-tree complex wavelet transform [21, 22] proposed by Kingsbury is an improvement to the conventional discrete wavelet transform (DWT). DWT is shift variant which leads to the significant change of wavelet coefficients at the output even with a small shift of the input signal. Additionally, DWT produces only three directionally selective subbands ($0^\circ, 45^\circ, 90^\circ$). Therefore, to overcome these limitations, DT-CWT was proposed which is shift invariant and improves directional resolution since it produces six directionally selective subbands ($\pm 15^\circ, \pm 45^\circ, \pm 75^\circ$). Moreover, DT-CWT is robust to noise, limited redundant and performs perfect reconstruction.

The DT-CWT uses two DWTs as shown in Fig. 1 (one dimensional (1-D) DTCWT). The real part of the transform is given by the first DWT while the imaginary part is given by the second DWT. The filter pair in the upper and lower DWT must be different otherwise no advantage is gained. Let $h_0(n)$ and $h_1(n)$ represent the filter pair for the upper tree while $g_0(n)$ and $g_1(n)$ represent the filter pair for the lower tree as shown in Fig. 1.

The 1-D DT-CWT decomposes an input signal $f(x)$ in terms of a complex shifted and dilated mother wavelet $\psi(x)$ and scaling function $\phi(x)$,

$$f(x) = \sum_{l \in \mathbb{N}} B_{j_0, l} \phi_{j_0, l}(x) + \sum_{j \geq j_0} \sum_{l \in \mathbb{N}} w_{j, l} \psi_{j, l}(x) \quad (11)$$

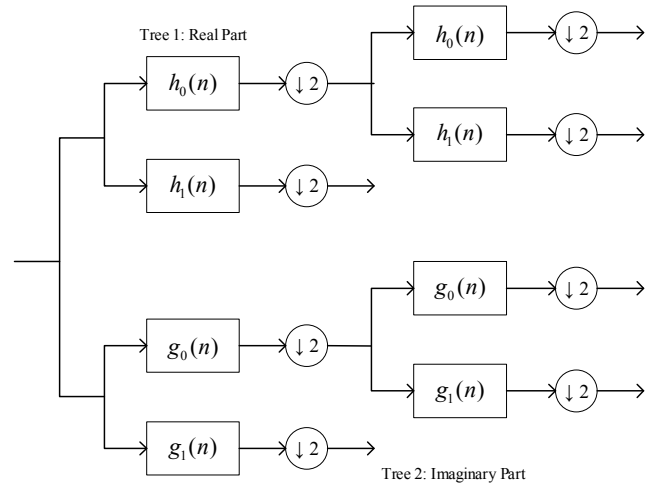


Fig. 1. 1-D dual-tree complex wavelet transform.

where N represents set of natural numbers, j_0 is the number of decomposition level, j and l are the index of shifts and dilations respectively, $B_{j_0, l}$ refers to the scaling coefficient and $w_{j, l}$ for the complex wavelet coefficients respectively. $\phi_{j_0, l}(x)$ is the scaling function computed as, $\phi_{j_0, l}(x) = \phi_{j_0, l}^r(x) + i\phi_{j_0, l}^i(x)$ and $\psi_{j, l}(x)$ is the complex wavelet function computed as, $\psi_{j, l}(x) = \psi_{j, l}^r(x) + i\psi_{j, l}^i(x)$, where the superscripts r and i represent the real and imaginary part respectively.

Similarly, in two dimensional (2-D) DTCWT, an image $f(x, y)$ is decomposed by complex scaling function and six complex wavelet functions as,

$$f(x, y) = \sum_{l \in \mathbb{N}^2} B_{j_0, l} \phi_{j_0, l}(x, y) + \sum_{\theta \in \beta} \sum_{j \geq j_0} \sum_{l \in \mathbb{N}^2} w_{j, l}^\theta \psi_{j, l}^\theta(x, y) \quad (12)$$

where $\theta \in \beta = \{\pm 15^\circ, \pm 45^\circ, \pm 75^\circ\}$ gives the directionality of the complex wavelet function. Hence, DT-CWT gives a complex-valued low pass subband and six complex-valued high pass subbands at every level of decomposition where each high pass subband represents one unique direction θ .

III. IMPLEMENTATION

In the proposed level set method, we obtain the iteration scheme by discretizing the partial differential equation (PDE) given by (8) as central finite differences. The binary step function is used for the initialization of level set function as it helps in easier emergence of new contours and faster curve evolution than the initialization with a signed distance map. The binary step function takes negative constant value $-c_0$ inside the region and positive constant value c_0 outside the region. In our experiments we use $c_0 = 2$.

In our work, we use Gaussian kernel K_σ with a scale parameter σ as a convolution kernel. The value of σ is selected as 10 for all the experiments. The convolution kernel can be constructed as a $w \times w$ mask, such that $w \geq 4\sigma + 1$. Therefore, we use a mask of size 41×41 . A smaller value of σ can be used, but it will require large number of iterations for accurate computations.

In our experiment, the two convolutions $K_\sigma * I$ and $K_\sigma * 1$ required to compute f_2 in (10) can be determined only once before the iterations as the evolution of level set function does not depend on them. But, the other two convolutions $K_\sigma * [H_\varepsilon(\phi)I]$ and $K_\sigma * H_\varepsilon(\phi)$ required for the computation of functions f_1 and f_2 in (10) needs to be computed at every iteration for evolving level set function. Similarly, $(\lambda_1 e_1 - \lambda_2 e_2)$ in (8) consists of three convolutions. However, one of them is not dependent on evolving level set function and hence can be computed only once before the iterations like in earlier case. Therefore, we need to compute four convolutions at each iteration for evolving level set function.

The level set function results in jagged output and also over segments the SN. Therefore, DT-CWT is used to address these issues and employed while evolving the level set function. At each scale, DT-CWT produces six directional subbands. Moreover, DT-CWT consists of two wavelets in each direction. Therefore, one wavelet can be considered as the real part while the other can be interpreted as the imaginary part of the complex-valued wavelet. In our experiments, we take the forward DT-CWT over 3 level of decomposition. DT-CWT is performed using different filter sets along the rows and columns. Oriented wavelets is obtained by performing sum and difference of subband images. Sum and difference operation is normalized by $1/\sqrt{2}$. Then, for the purpose of smoothing, we apply thresholding to high frequency wavelet coefficients through all scales and subbands. The threshold value is determined by the heuristic approach. Finally, we take inverse DT-CWT to obtain the smooth image contour and also to resolve the over-segmentation.

IV. RESULTS AND DISCUSSION

The proposed method of combining level set method with DT-CWT for accurate segmentation of SN requires various parameters to be specified. We use the following parameters for the level set method for various MR images: $\lambda_1 = 1.0$, $\lambda_2 = 2.0$, $\mu = 1$, $\nu = 0.003 \times 255 \times 255$, $\varepsilon = 1.0$ and $\sigma = 10.0$.

The proposed method is applied to the data obtained from different age groups including young, middle-aged and elderly participants. The segmentation results of our proposed method along with the comparison to the level set methods [13, 14] is shown in Fig. 2. The level set method based on the RSF model is referred as Method II while the level set method based on local intensity clustering property is referred as Method III. The area included within the red contours in the sample scans 1-5, represent the final

segmentation result of SN using our proposed method along with the level set methods.

An experienced radiologist performed the subjective evaluation for the analysis of different methods. The subjective evaluation score is shown in Table I. The proposed method obtained the highest subjective score in comparison to other two methods. The radiologist liked the smooth result of the proposed methodology and stated that it enclose better SN in comparison to method II and method III. The results produced by the method proposed in this work is closer to the manual segmentation than the level set methods which constantly overestimated and underestimated SN as shown in the Fig. 2.

The proposed method of combining level set method and DT-CWT works well for the segmentation of smaller brain nuclei like SN. The level set method proposed in this work use the local image intensities rather than the global intensities and also avoids the need of re-initialization. However, level set method independently cannot segment the desired region. Hence, DT-CWT is used for accurate segmentation along with level set method. DT-CWT is capable of removing holes, solve the over-segmented regions and smooth the rough output resulting from the level set method, and give the desired region of interest segmentation.

The level set methods (Method II and Method III) is employed for the comparative analysis in our proposed work. But, the level set method is not capable of segmenting SN accurately because of the similar intensity values between the region of interest and the adjacent areas. It constantly overestimates and underestimates the region of interest as shown in Fig. 2. Additionally, the jagged output, holes and the smaller areas resulting out of level set method do not make anatomic sense according to clinicians perspective.

Medical imaging applications comes with an inherent problem of selecting an appropriate ground truth image which we come across as well. We are working with our radiologist and neuropathologist to generate the ground truth model. Therefore selecting an appropriate ground truth and performing quantitative analysis will be the future work. Moreover, improving the proposed methodology and making it more robust will be the future direction and goal of this research.

V. CONCLUSION

In this paper, we have presented an improved segmentation algorithm for SN by combining level set method and DT-CWT. The level set method uses the local image information for the segmentation of SN. However, it is unable to perform accurate segmentation of SN. It repeatedly overestimates SN and creates small areas and holes along with the jagged output. Therefore, to overcome these limitations, DT-CWT is proposed in our work which results in smooth and accurate segmentation of SN. The subjective evaluation performed by the radiologist supports our claim and validates the proposed methodology. SN segmentation performed using the proposed method were closer to manual segmentation than the level set methods. Our future work will be focused on performing volumetric analysis and morphometric variability of SN which will be useful to detect and study PD characteristics and progression.


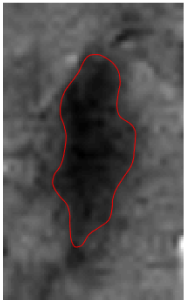
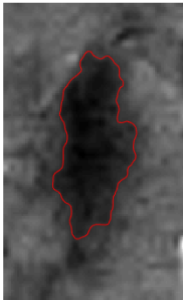
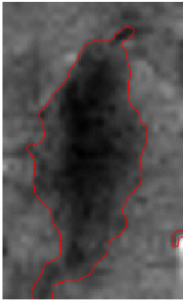
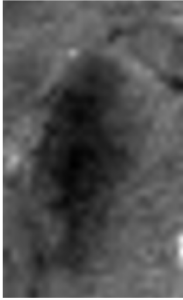
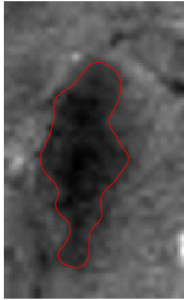
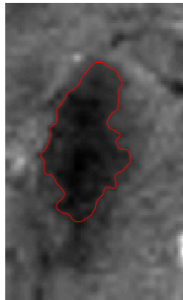
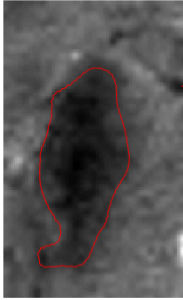

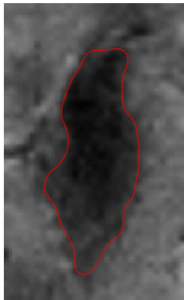
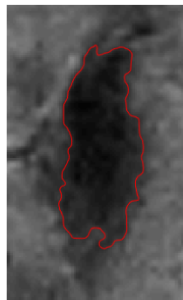
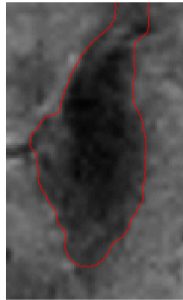


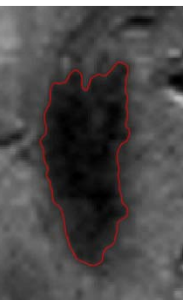

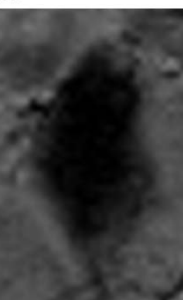

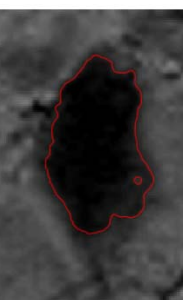
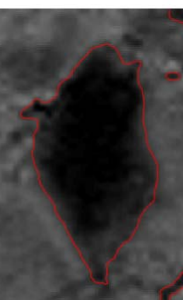
Original Image	Proposed Method (Method I)	Level set method based on mi- -nimization of region-scalable fitting energy (Method II)	Level set method in the presen- -ce of intensity inhomogeneitie- -s with application to MRI (Method III)
Scan 1 			
Scan 2 			
Scan 3 			
Scan 4 			
Scan 5 			

Fig. 2. Comparison of segmentation results of our proposed method with different methods.

TABLE I. SUBJECTIVE EVALUATION SCORES

SCAN NUMBER	RATINGS (1-5)		
	Method I	Method II	Method III
Scan 1	3	2	1
Scan 2	3	1	3
Scan 3	3	2	2
Scan 4	3	2	3
Scan 5	4	2	2

Note: 1: Lowest
5: Highest

REFERENCES

- [1] J. M. Fearnley, and A. J. Lees, "Ageing and Parkinson's disease: substantia nigra regional selectivity," *Brain*, vol. 114 (Pt 5), pp. 2283-301, Oct, 1991.
- [2] W. R. B. Brain, and J. N. Walton, *Brain's Diseases of the nervous system*, 8th ed., Oxford Eng. ; New York: Oxford University Press, 1977.
- [3] B. Hallgren, and P. Sourander, "The effect of age on the non-haemin iron in the human brain," *J Neurochem*, vol. 3, no. 1, pp. 41-51, Oct, 1958.
- [4] E. Sofic, W. Paulus, K. Jellinger, P. Riederer, and M. B. Youdim, "Selective increase of iron in substantia nigra zona compacta of parkinsonian brains," *J Neurochem*, vol. 56, no. 3, pp. 978-82, Mar, 1991.
- [5] R. A. Menke, S. Jbabdi, K. L. Miller, P. M. Matthews, and M. Zarei, "Connectivity-based segmentation of the substantia nigra in human and its implications in Parkinson's disease," *Neuroimage*, vol. 52, no. 4, pp. 1175-80, Oct 1, 2010.
- [6] Y. Xiao, L. Bailey, M. M. Chakravarty, S. Beriault, A. F. Sadikot, G. B. Pike, and D. L. Collins, "Atlas-Based Segmentation of the Subthalamic Nucleus, Red Nucleus, and Substantia Nigra for Deep Brain Stimulation by Incorporating Multiple MRI Contrasts," *Information Processing in Computer-Assisted Interventions*. pp. 135-145.
- [7] C. Haegelen, P. Coupe, V. Fonov, N. Guizard, P. Jannin, X. Morandi, and D. L. Collins, "Automated segmentation of basal ganglia and deep brain structures in MRI of Parkinson's disease," *Int J Comput Assist Radiol Surg*, vol. 8, no. 1, pp. 99-110, Jan, 2013.
- [8] Y. Xiao, P. Jannin, T. D'Albis, N. Guizard, C. Haegelen, F. Lalys, M. Verin, and D. L. Collins, "Investigation of morphometric variability of subthalamic nucleus, red nucleus, and substantia nigra in advanced Parkinson's disease patients using automatic segmentation and PCA-based analysis," *Hum Brain Mapp*, vol. 35, no. 9, pp. 4330-44, Sep, 2014.
- [9] J. Kim, C. Lenglet, Y. Duchin, G. Sapiro, and N. Harel, "Semiautomatic segmentation of brain subcortical structures from high-field MRI," *IEEE J Biomed Health Inform*, vol. 18, no. 5, pp. 1678-95, Sep, 2014.
- [10] B. Li, C. Jiang, L. Li, J. Zhang, and D. Meng, "Automated Segmentation and Reconstruction of the Subthalamic Nucleus in Parkinson's Disease Patients," *Neuromodulation*, vol. 19, no. 1, pp. 13-9, Jan, 2016.
- [11] E. Visser, M. C. Keuken, B. U. Forstmann, and M. Jenkinson, "Automated segmentation of the substantia nigra, subthalamic nucleus and red nucleus in 7 T data at young and old age," *Neuroimage*, vol. 139, pp. 324-336, Oct 1, 2016.
- [12] T. Guo, Y. Song, J. Li, M. Fan, X. Yan, A. He, D. Huang, C. Shen, G. Zhang, and G. Yang, "Seed point discontinuity-based segmentation method for the substantia nigra and the red nucleus in quantitative susceptibility maps," *J Magn Reson Imaging*, Mar 31, 2018.
- [13] C. Li, C. Y. Kao, J. C. Gore, and Z. Ding, "Minimization of region-scalable fitting energy for image segmentation," *IEEE Trans Image Process*, vol. 17, no. 10, pp. 1940-9, Oct, 2008.
- [14] C. Li, R. Huang, Z. Ding, J. C. Gatenby, D. N. Metaxas, and J. C. Gore, "A level set method for image segmentation in the presence of intensity inhomogeneities with application to MRI," *IEEE Trans Image Process*, vol. 20, no. 7, pp. 2007-16, Jul, 2011.
- [15] B. U. Forstmann, M. C. Keuken, A. Schafer, P.-L. Bazin, A. Alkemade, and R. Turner, "Multi-modal ultra-high resolution structural 7-Tesla MRI data repository," *Scientific Data*, vol. 1, pp. 140050, 12/09/online, 2014.
- [16] S. Osher, and J. A. Sethian, "Fronts propagating with curvature-dependent speed: Algorithms based on Hamilton-Jacobi formulations," *Journal of Computational Physics*, vol. 79, no. 1, pp. 12-49, 1988/11/01/, 1988.
- [17] T. F. Chan, and L. A. Vese, "Active contours without edges," *Ieee Transactions on Image Processing*, vol. 10, no. 2, pp. 266-277, Feb, 2001.
- [18] D. Mumford, and J. Shah, "Optimal Approximations by Piecewise Smooth Functions and Associated Variational-Problems," *Communications on Pure and Applied Mathematics*, vol. 42, no. 5, pp. 577-685, Jul, 1989.
- [19] C. M. Li, C. Y. Kao, J. C. Gore, and Z. H. Ding, "Implicit active contours driven by local binary fitting energy," *2007 Ieee Conference on Computer Vision and Pattern Recognition, Vols 1-8*, pp. 339-+, 2007.
- [20] S. G. Mallat, *A wavelet tour of signal processing*, 2nd ed., San Diego: Academic Press, 1999.
- [21] N. Kingsbury, "The Dual-Tree Complex Wavelet Transform: A New Technique For Shift Invariance And Directional Filters."
- [22] N. Kingsbury, "Complex Wavelets for Shift Invariant Analysis and Filtering of Signals," *Applied and Computational Harmonic Analysis*, vol. 10, no. 3, pp. 234-253, 2001/05/01/, 2001.